(Received 3 June 2025, Accepted 11 July 2025, Scheduled 9 August 2025)

Development of a Half-Sphere Microwave Absorber with Enhanced Performance

Aya R. Thanoon and Khalil H. Sayidmarie*

Department of Communication Engineering, College of Electronics Engineering, Ninevah University, Mosul, Iraq

ABSTRACT: The paper proposes a microwave absorber in the form of half-spheres placed on a base layer as an alternative to the conventional pyramidal shape. The performance of the absorber is investigated, focusing on the influence of the diameter of the half-sphere, permittivity, loss tangent, and angle of the incident wave and its polarization. The study also evaluates the case when the absorber is backed by a conducting plate that is required for shielded anechoic chambers. Simulation results using CST Microwave suite indicate that increasing loss tangent enhances absorption while decreasing permittivity reduces reflectivity. The proposed absorber offers low sensitivity of reflection concerning the angle of incidence due to the symmetry of the spherical surface. The obtained results were confirmed by simulations using the HFSS software. The results show that the proposed absorber has a competitive performance with the pyramidal absorber of the same total thickness.

1. INTRODUCTION

The use of radio frequency (RF) and microwave devices and systems is ever increasing in volume and in the risk of electromagnetic (EM) interference and radiation leakage, which pose threats to the performance of these devices as well as human health. Therefore, the research on EM absorbers that can reduce these effects has grown steadily, aiming to offer materials and designs of absorbers that are characterized by being thin, lightweight, and covering a wide frequency band. The use of absorbers aims to reduce or eliminate the reflection, transmission, and scattering of microwave radiation, thereby minimizing interference or reducing the risk of detection. On the other hand, absorbers are essential parts of anechoic chambers used for testing RF devices and systems.

The efforts to enhance the performance of microwave absorbers have been in two main fields: firstly, the development of a suitable and cheap lossy material to fabricate the absorber. Secondly, the design of a proper surface profile of the absorber, and thickness is required to offer low reflection and adequate absorption at a reasonable thickness. While the first line of research aims to offer higher loss per unit length of the absorber, the surface profile can reduce the initial reflection right at the surface of the absorber, where the incident EM waves meet the absorber surface [1–3]. The materials that can be used for the fabrication of absorbers must have an adequate level of loss, such as lossy dielectric materials, lossy magnetic materials, a combination of both, or hybrid absorbers (a composite of two different materials), and structures showing metamaterial effects. Absorbers based on metamaterial effect can offer very thin designs in terms of wavelength but have either narrow or multiple bands such as the triple band absorber presented in [4] that works at microwave frequencies, and in [5] which showed hepta absorbing bands in the THz frequencies. To optimize the metamaterial absorber designs for Terahertz applications machine learning techniques have been used [6].

Certain agricultural leftovers, such as coconut coir, banana leaves, other byproducts, and ceramic materials, have been investigated as alternatives to foams in the construction of absorbers in the microwave frequency range [7–11]. Kaur et al. employed rice husk and a mixture of rice husk and coal to construct pyramid microwave absorbent structures, which produced the mean reflection of -30 dB and -40 dB, respectively [12]. The work aiming to develop lossy dielectric materials for deployment into microwave absorbers continues, where ferrite-based and carbon-based materials are being developed to achieve better performance [1–3, 13].

The shape of an absorber is an important factor that influences the level of reflection since it forms the boundary between the air and the lossy material of the absorber where the EM wave is incident. At this interface, the reflection is determined according to boundary conditions and the law of reflection. Pyramidal absorbers were extensively used as they usually offer a gradual change from air to the absorbing material. The performance of pyramidal and truncated pyramidal absorbers with various permittivity values constructed of solid, hollow, or coated materials was investigated in [14], and it was shown that higher permittivity corresponded to somewhat higher reflection. In [15], three shapes for the base of a pyramid absorber, namely triangle, isosceles, and square, fabricated from rice husks, were investigated across the frequencies 1–20 GHz, and the obtained results showed that the form of a pyramid base could impact the performance of the absorber. Eight polygon-based pyramidal shapes, i.e., triangle, tetragon (or square), pentagon, hexagon, heptagon, octagon, nonagon, and decagon, as

* Corresponding author: Khalil Hassan Sayidmarie (kh.sayidmarie@uoninevah.edu.iq).

well as a circular cone, were investigated using a material with a permittivity of 2.9. The comparison considered the surface area of the absorber, and it was found that the triangular base shape achieved better results [16]. While the triangular shape has the lowest surface area that seems to absorb less power, the reduced reflection can be attributed to multiple reflections between adjacent pyramids. In [17], a hexagon-based pyramid constructed from banana leaves, rice husks, and rice straws was examined at frequencies varying from 0.01 to 20 GHz. The obtained results for 13 cm thick absorbers showed reflection levels of -35 dB, -39 dB, and -38 dB, respectively. When the pyramid was truncated, the reflection coefficients slightly deteriorated. A derived version of the pyramid is wedge shape, where the height can be varied to achieve better performance from this extra degree of design freedom. In [18], the performance of conventional, concave, and convex surfaces was compared, and it was shown that the reflection from a wedge-shaped absorber is better than a concave-shaped one, while a convex-shaped absorber has the best results.

Pyramidal shape was also adopted in the form of discrete staggered layers, as in [19], where circular disks were combined to form a cone. The design exhibited a metamaterial effect as each layer comprised a conducting circle on a dielectric substrate. The multi-layer structure increases the narrow bandwidth of the single-layer design, even at small thicknesses, but the achieved reflection coefficient was around -15 to -20 dB.

Hollow Pyramidal Absorbers (HPAs) can offer an additional degree of freedom to enhance bandwidth performance by furnishing hollow sections of different sizes [20]. These sections offer other resonance frequencies and thus can extend the absorption band. In [21], isosceles triangular slots achieved the absorptivity of -26.32 dB across L to X frequency bands, while in [20], a triangular-slotted hollow pyramidal absorber using the Sierpinski principle showed improved performance. In [22], a honeycomb structure made of dielectric material coated by a conductive material was investigated as a microwave absorber. The obtained reflection coefficient for an 8.5 cm thick absorber backed by a conducting plane was around -20 dB for the frequency range 6–18 GHz. These results are larger than those achievable by conventional absorbers though the honeycomb absorber was of smaller thickness. The reason can be attributed to the fact that in the honeycomb structure most of the absorber volume is air which does not contribute to the absorption.

Another simple shape absorber is planar or flat absorber, where a lossy dielectric material at a certain thickness can show low reflectivity at a narrow band of frequencies. To enhance the bandwidth of the single-layer absorber, multi-layer configurations have been proposed, where the thickness and permittivity of the layers are optimized to achieve lower reflection across a wider band of frequencies [23, 24]. Five or more layers of different permittivities and permeabilities, having well-optimized values, are needed to achieve acceptable reflectivity across one of the microwave bands [25]. While these designs can easily offer a relatively thin absorber, the achieved bandwidth is much smaller than that offered by pyramidal absorbers.

It has been shown recently that to achieve low reflection and adequate absorption, the relative permittivity of the material used for the absorber must be moderate, while the loss tangent must be high to attain the desired absorption [26]. The magnetic properties of the absorber material can also be utilized to reduce the reflection, and the best designs are achieved when the magnetic and dielectric parameters of the absorber material are properly chosen [26]. The surface profile of the absorber should be such that the absorber material is introduced gradually to reduce initial reflection at the air-absorber interface. Therefore, pyramidal and wedge shapes were favorites in the design of absorbers, and still other surface profiles may offer lower reflection.

This study proposes employing a spherical profile in the design of microwave absorbers, as the spherical surface offers a gradual and smooth introduction of the absorber material. Moreover, due to the spherical symmetry, the reflection from the spherical surface is independent of the angle of incidence. The proposed absorber has the shape of a half-sphere placed on a planar base layer. The influences of the absorber's height, base thickness, permittivity, loss tangent of the absorber material, the angle of incidence, and polarization of the applied EM wave have been analyzed. Furthermore, the paper investigates the case where the absorber is backed by a conducting plate that is employed in shielded anechoic chambers. The paper is organized as follows. Section 2 analyzes the reflection of EM wave from lossy dielectric spheres. Section 3 investigates the performance of the proposed absorber using Computer Simulation Technology (CST) software and explores the influence of the various parameters of the absorber. Section 4 investigates the performance of absorbers backed by conducting plates. Section 5 compares the performance of the proposed hemisphere absorber with a pyramidal absorber having the same square base layer and overall thickness, while Section 6 compares the results obtained from CST and High Frequency Structure Simulator (HFSS) software packages. Section 7 compares the obtained results with those presented in other published works. The drawn conclusions are presented in Section 8.

2. SCATTERING AND REFLECTION FROM DIELECTRIC SPHERES

The scattering of electromagnetic waves from a dielectric sphere of permittivity ε depends on the ratio D/λ between the diameter of the sphere D and the wavelength λ of the incident wave. This ratio is expressed as $ka = 2\pi a/\lambda$, where k is the wave number or the phase constant in units of radians/meter, and $a = D/2$ is the radius of the sphere. It is well established that when $ka \ll 1$ or $D/\lambda \ll 1/\pi$, the scattering is given by the Rayleigh law, while when this condition is not satisfied, the scattering is given by the Mie relation. It can be shown that the relative magnitude of the scattered field under Rayleigh conditions for a nonmagnetic dielectric sphere can be given by [27]:

$$SS = k^2 a^3 \frac{(\varepsilon - \varepsilon_0)}{(\varepsilon + 2\varepsilon_0)} \sin(\theta) \tag{1}$$

where θ is the direction angle from the electric field, and $\theta = \pi/2$ for forward scattering and $\theta = 3\pi/2$ for backward scat-

TABLE 1. Comparison of the frequency at which maximum reflection occurs and the sphere diameter in terms of the wavelength for the cases shown in Fig. 1.

Sphere diameter D [cm]	Frequency for max. $\|S_{11}\|$ [GHz]	λ_0 [cm]	D/λ_0	λ_e [cm]	D/λ_e	$\pi D/\lambda_e$
3	2.6	11.5	0.26	9.4	0.31	1.00
4	1.9	15.7	0.25	12.8	0.31	0.97
5	1.5	20	0.25	16.3	0.30	0.96

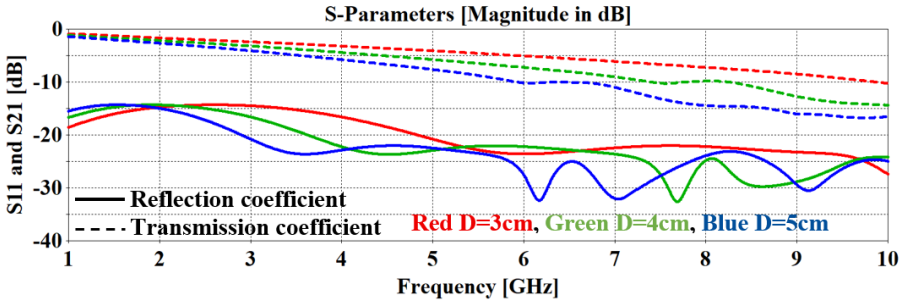

FIGURE 1. Variation of the reflection coefficient $|S_{11}|$ and transmission coefficient $|S_{21}|$ for a sphere of 3, 4, and 5 cm diameter, $\varepsilon_r = 1.5$ and $\tan\delta = 0.5$.

tering or reflection. The above relation shows that the reflection increases as the permittivity of the sphere departs from the free space value ε_0. Moreover, the reflection is directly proportional to the 3rd power of the size (radius) of the sphere, while it is inversely proportional to the square of the wavelength as $k^2 = 4\pi^2/\lambda^2$.

To assess the reflection of electromagnetic waves from dielectric spheres, CST Studio Suite 3D EM analysis software package was used to run a simulation study. The case where a 4 cm diameter sphere having a permittivity of $\varepsilon_r = 1.5$ and loss tangent $\tan\delta = 0.5$ was simulated in the unit cell boundary conditions. The cell size was 6×6 cm, and the obtained scattering parameters are shown in Fig. 1. For each sphere size, maximum reflection occurs at a certain frequency, then the reflection coefficient drops as the frequency of the incident wave is increased. It can also be noticed that larger sphere sizes lead to a slightly lower reflection coefficient. The frequency corresponding to the highest reflection decreases as the sphere diameter is increased. The relation between the sphere diameter and the wavelength in air λ_0 and that inside the sphere λ_e are detailed in Table 1. The table shows that maximum reflection occurs when the circumference of the sphere equals the effective wavelength inside the sphere (i.e., when $\pi D/\lambda_e = 1$). The reflection drops steadily as the frequency increases. The transmission coefficient decreases steadily with the frequency due to the increased loss in the sphere, and a larger sphere results in a lower transmission coefficient.

2.1. Distribution of the Power Density in the Sphere

Examination of the distribution of the power density in the lossy dielectric sphere gives good insight into where the power is deposited and how the various parts of the sphere share the lost power. The calculated power density at frequencies of 1 GHz, 5 GHz, and 10 GHz is shown in Fig. 2. The results demonstrate that the maximum power density is on the sphere side that is facing the incident wave, and the power density decreases towards the center of the sphere and its back half. Moreover, as the frequency was increased from 1 GHz to 5 GHz and to 10 GHz, the values of the maximum power increased from 5699 to 21883 and 42394 W/m^3, respectively. The region of higher power density covers a larger portion of the sphere as the frequency of the incident wave is increased indicating higher absorption.

3. THE PROPOSED HALF-SPHERE ABSORBER

The results of the previous section showed that the loss of power in the sphere is larger across its half that is facing the source of the incident wave. Thus, it is suggested here to build an absorber formed of a half sphere placed on a square base. The half-sphere shape can offer a gradual introduction of the material into the air as the pyramidal shape does. Moreover, the spherical symmetry of the sphere results in less dependence on the angle of incidence, which is a desired property for absorbers. The sphere has a rounded surface, with neither sharp angles nor fast shape changes, resulting in reflection at edges and discontinuities.

Figure 3 shows the construction of the proposed absorber, which was modeled using the CST 3D EM analysis software package. The EM wave was incident at port 1, where the reflection coefficient S_{11} was determined, while the transmission coefficient S_{21} was determined at port 2. The unit cell approach was adopted for modelling the absorber, and the frequency domain solver was used for the calculations under the unit cell boundary conditions. The unit cell is composed of a half-sphere of diameter D placed on a $D \times D$ base of b cm thickness. The effects on the reflection coefficient of the various absorber parameters, such as relative permittivity εr, loss tangent $\tan\delta$, sphere diameter D, the angle Φ of the incident

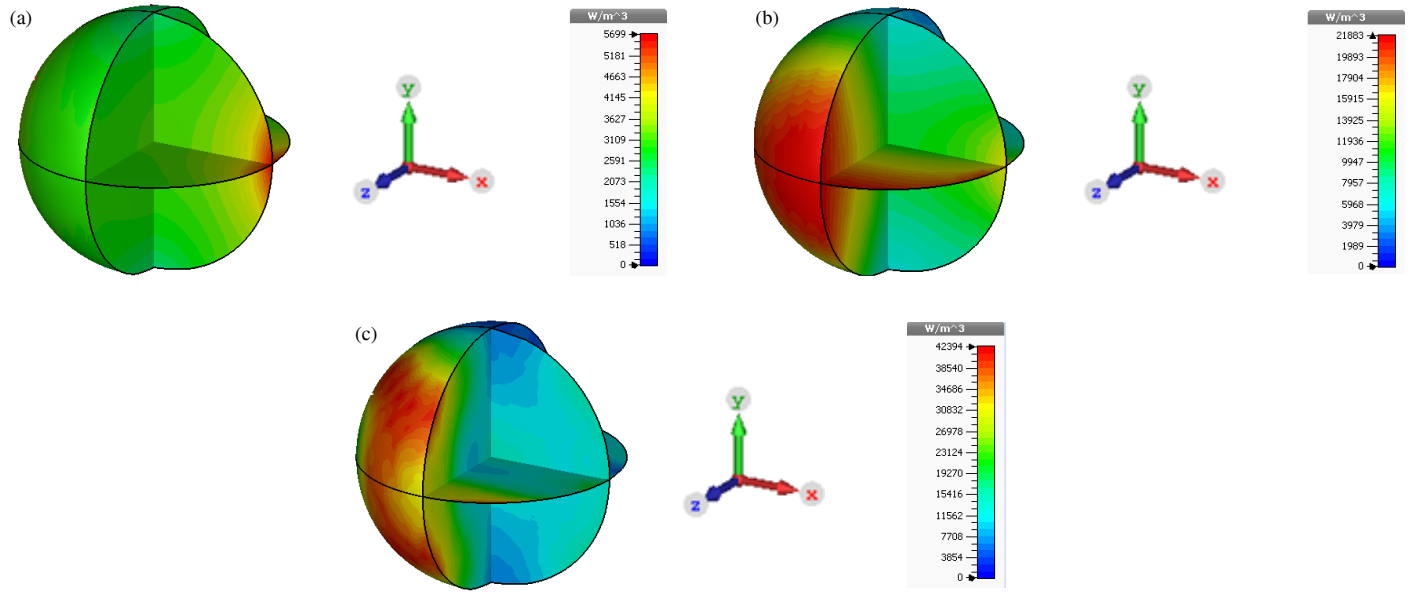

FIGURE 2. Power density distribution in a sphere of 4 cm diameter, with $\varepsilon_r = 1.5$, and $\tan\delta = 0.5$ for frequencies (a) 1 GHz, (b) 5 GHz, and (c) 10 GHz subjected to an incident plane wave propagating along the negative Z-axis. (a) $f = 1$ GHz. (b) $f = 5$ GHz. (c) $f = 10$ GHz.

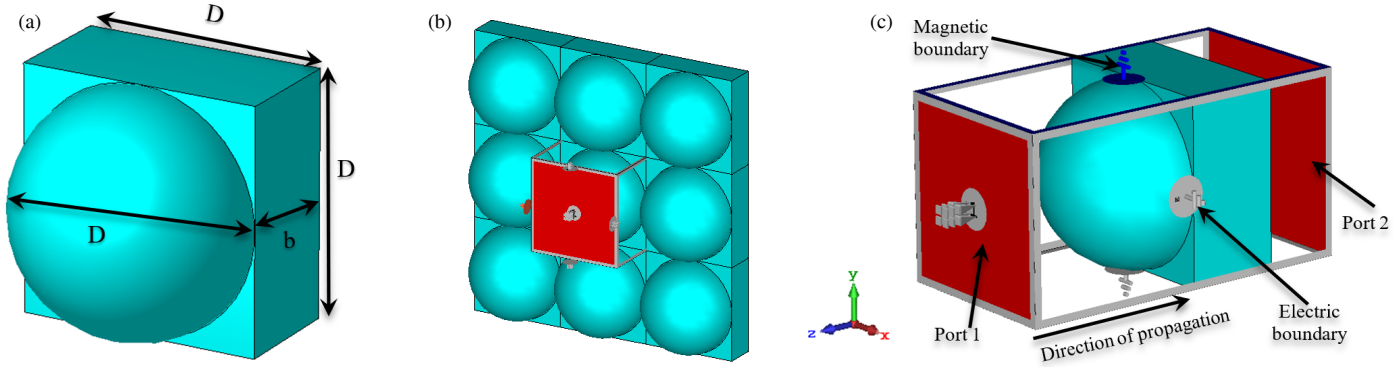

FIGURE 3. The simulation model in the CST microwave suit showing the unit cell configuration.

wave, and its polarization, were investigated. The obtained results are presented and discussed in the following subsections.

3.1. Effect of Relative Permittivity

The permittivity of the absorber material is an important factor in determining the reflection coefficient. Fig. 4 shows the variation of the reflection coefficient of the absorber with frequency for three values of relative permittivity ε_r, 1.5, 2.5, and 3.5, when the loss tangent was fixed at $\tan\delta = 0.5$. The results indicate that the reflection increases with the relative permittivity for frequencies up to about 8 GHz, and then reflection at a higher permittivity of 3.5 shows larger values than the cases of lower permittivity. For the three cases of permittivity, the reflection decreases to small values at frequencies around 5 GHz.

3.2. Effect of the Loss Tangent

The loss tangent $\tan\delta$ of the absorber material is an important factor in absorbing the EM wave that penetrates the absorber material, thus, it influences the level of the wave that leaves the absorber as a reflected wave. Fig. 5 shows the level of the reflection coefficient for $\tan\delta$ values of 0.01, 0.1, and 0.5, while the diameter was kept at $D = 10$ cm, and $\varepsilon_r = 1.5$. It is clearly seen that higher values of loss tangent $\tan\delta$ lead to lower reflection. The effect is more pronounced at higher frequencies. An increase in the loss tangent leads to a greater ability of the material to convert electromagnetic waves into heat, thereby reducing the reflected energy. This explains why the reflection coefficient decreases as the loss tangent increases.

3.3. Effect of the Sphere Diameter

The height of the absorber is determined by the diameter of the sphere D and base thickness b. The total thickness of the absorber, and thus the total volume of the absorbing material, is governed by these two values. For a fixed base thickness, a smaller diameter of the sphere means a smoother introduction of the absorber material into the air, which will lead to reduced reflection. Fig. 6 shows the effect of the sphere diameter D on the achieved reflection of the absorber when D was varied from

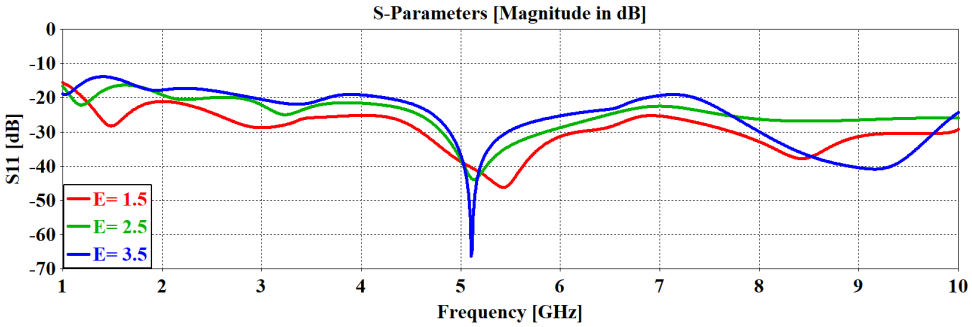

FIGURE 4. Variation of the reflection coefficient $|S_{11}|$ with frequency for the half-sphere absorber (diameter $D = 10$ cm, base thickness $b = 5$ cm, and $\tan\delta = 0.5$) for various values of ε_r.

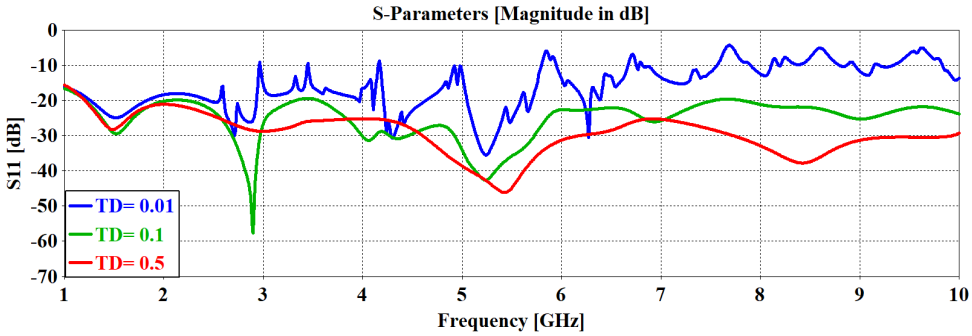

FIGURE 5. Variation of the reflection coefficient $|S_{11}|$ with frequency for a half-sphere absorber with a diameter $D = 10$ cm and $\varepsilon_r = 1.5$, for various values of $\tan\delta$.

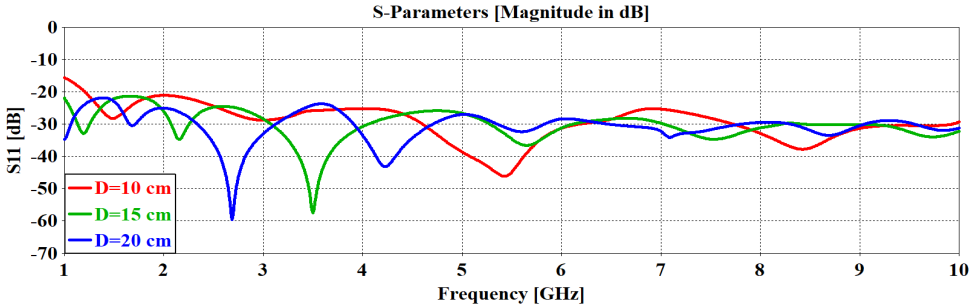

FIGURE 6. Variation of the reflection coefficient $|S_{11}|$ with frequency for the absorber with $\varepsilon_r = 1.5$, $\tan\delta = 0.5$, and a base thickness of 5 cm for sphere diameters of 10, 15, and 20 cm.

10, 15, and 20 cm while fixing values of $\varepsilon_r = 1.5$, $\tan\delta = 0.5$. For the above values of the sphere diameter, the total thickness of the absorber is 10, 12.5, and 15 cm, respectively. The obtained results show that the increase in the sphere diameter slightly reduces the reflection coefficient, which is due to the increase in the total thickness of the absorber. It is also noticed that the frequency at which maximum reflection occurs decreased as the sphere diameter was increased. Moreover, the reflection coefficient is less than -22 dB across the frequency range of 1 GHz to 10 GHz, which means that an average reflection level of -22 dB/15 cm (-1.47 dB/cm) has been achieved.

The obtained results also show that for the sphere diameters of 10, 15, and 20 cm, the minimum reflection occurs at a frequency of 5.428 GHz, 3.5 GHz, and 2.683 GHz, respectively. At each of these frequencies, the diameter D of the sphere is almost twice of the effective wavelength λ_e at the corresponding frequency, or the thickness of the half-sphere is equal to the effective wavelength as detailed in Table 2.

3.4. Effect of Base-Layer Thickness

The base layer of the absorber is an integral and important part of the absorber and can influence its performance. Fig. 7 shows the simulation results for three absorbers with base thicknesses of 5, 10, and 15 cm. The general conclusion is that a thicker base layer leads to a lower reflection coefficient. The increase in the thickness by 3-fold (from 5 cm to 15 cm) has resulted in about 10 dB reduction in the reflection coefficient. This modest decrease in the reflection coefficient can be attributed to the half-sphere, which is the first region that faces the incident wave and thus has more influence on the reflection coefficient. The thickness of the base layer also influences the transmis-

TABLE 2. Parameters of the absorber at the frequency that gives the minimum reflection coefficient.

D [cm]	Frequency [GHz] at which $\lvert S_{11}\rvert$ is min	λ_0 [cm]	λ_e [cm]	D/λ_e
10	5.428	5.52	4.51	2.21
15	3.5	8.57	6.99	2.14
20	2.683	11.18	9.12	2.19

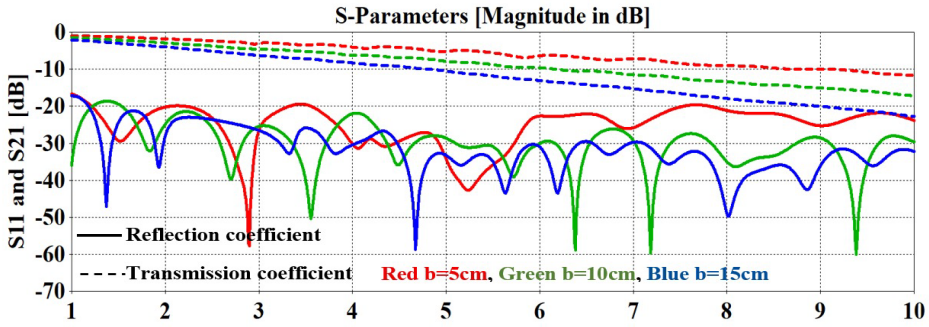

FIGURE 7. The variation of the reflection coefficient $|S_{11}|$ and transmission coefficient $|S_{21}|$. With a frequency for sphere diameter of 10 cm, $\varepsilon_r = 1.5$, and $\tan\delta = 0.1$ at normal incidence, and various base thicknesses of 5, 10, and 15 cm.

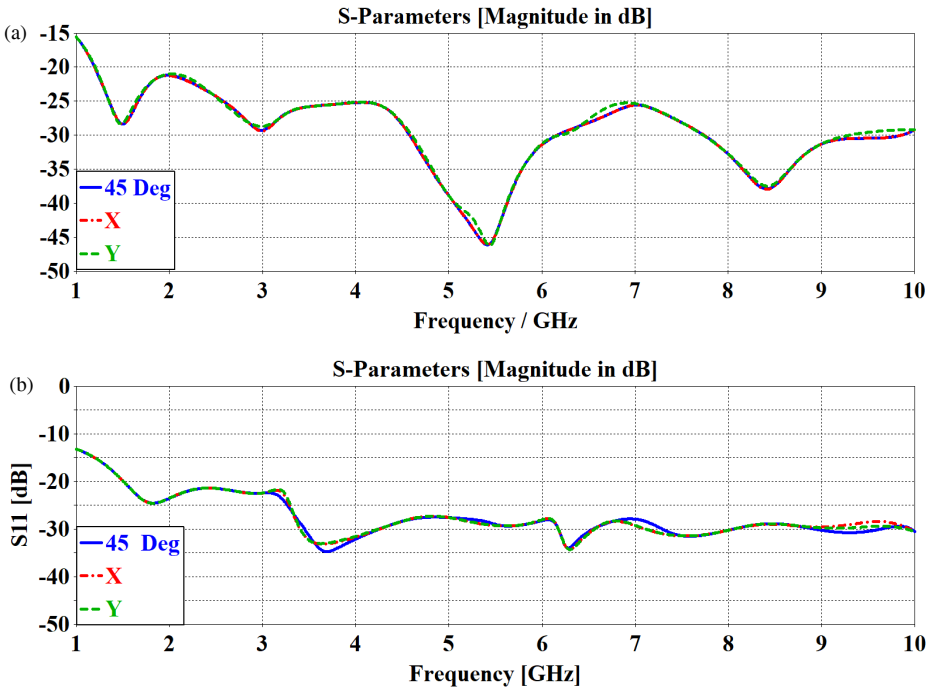

FIGURE 8. The reflection response of the proposed absorber at normal incidence, when the electric field is oriented along the X-axis Y-axis, and at 45°. (a) half-sphere absorber, and (b) pyramidal absorber.

sion coefficient, as demonstrated in Fig. 7, which shows that the transmission coefficient at 10 GHz dropped by about 10 dB when the base thickness was increased from 5 cm to 15 cm.

3.5. Effect of the Polarization and Angle of Incidence

In the investigated cases in the previous sections, the EM wave was assumed to be normally incident on the absorber, and the electric field is directed along the X-axis. The polarization sensitivity is shown in Fig. 8, which demonstrates that the absorber response is essentially the same for normal incidence where the electric field is oriented at X-axis, Y-axis, and at 45°. The figure also shows the performance of an equalsized pyramidal absorber, which indicates a similar trend, although the pyramidal absorber shows slightly larger deviations among the three polarizations. These results can be attributed to the symmetry of both absorbers with respect to the X- and Y-axes, and that the

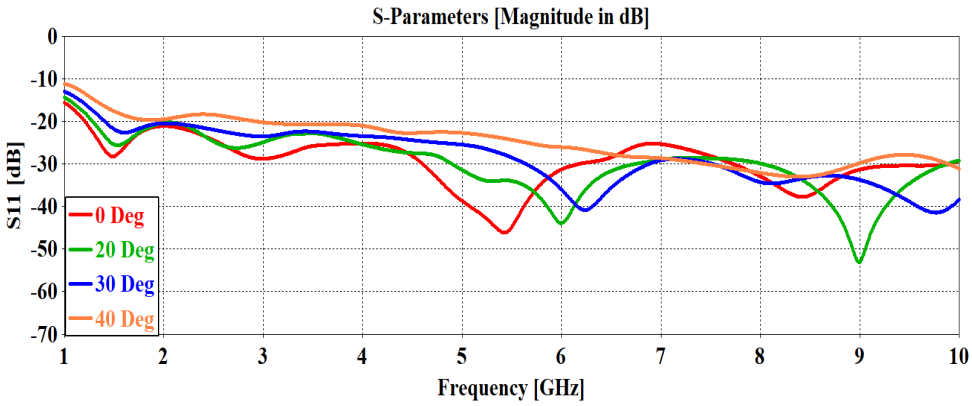

FIGURE 9. Variation of the reflection coefficient $|S_{11}|$ with frequency for the half-sphere absorber with a sphere diameter of 10 cm, base thickness = 5 cm, $\varepsilon_r = 1.5$, and $\tan\delta = 0.5$, at various incidence angles ($0°$, $20°$, $30°$, $40°$).

half-sphere geometry provides better symmetry than the pyramidal square base.

While the normal incidence is a special case, the oblique incidence at a certain angle is the general one. The reflection coefficient depends on the incidence angle with respect to the absorber surface as well as the properties of the absorber material. In general, microwave absorbers that are usually used in anechoic chambers exhibit increased reflection at oblique incidence, especially for angles larger than $40°$. This means that an appreciable portion of the incident wave is reflected back instead of being absorbed. The effect of the incidence angle was investigated using proper settings in the CST software. Fig. 9 shows the effect of changing the angle of incidence on the proposed absorber while fixing the other parameters at a sphere diameter $D = 10$ cm, $\varepsilon_r = 1.5$, $\tan\delta = 0.5$, and base thickness $b = 5$ cm. The results show that the reflection is slightly affected by the angle of incidence up to $30°$, while there is a few dB increase at the angle $40°$ for some of the frequencies in the shown range. However, at angles larger than $40°$, the reflection starts to increase above -20 dB. This finding was reported in [26, 28] where a 10 dB or more increase in the reflection was reported for incidence angles larger than $40°$, while in [29] more than 20 dB increase was reported. Table 3 compares the average reflection coefficient at various incidence angles for the half-sphere absorber to those obtained from an equal-size pyramidal absorber of the same material. The proposed absorber performs better for angles up to $20°$, then the two absorbers compete at higher angles, where the pyramidal absorber shows lower reflection, while the large angle performance of both declines.

TABLE 3. Comparison of the average reflection coefficient $|S_{11}|$ from the pyramidal absorber and an equal-sized pyramidal absorber at various incidence angles. $H = b = 5$ cm, $\varepsilon_r = 1.5$, and $\tan\delta = 0.5$.

Incidence angle	Half-sphere	Pyramidal
$0°$	-29.5	-27.5
$20°$	-29.7	-30.3
$30°$	-28.3	-29.1
$40°$	-24.9	-27.2
$50°$	-20.7	-21
$60°$	-16	-18.3
$70°$	-9.5	-10.3

3.6. Sensitivity of the Absorber to Tolerances in the Dimensions

The absorber's sensitivity to the tolerance in design dimensions was assessed by running simulations under some errors in the dimensions. Fig. 10 shows the obtained results under $\pm 5\%$ errors in the sphere diameter and base thickness. The reflection coefficient shows no appreciable sensitivity to the base thickness, as the reflection is a process at the face of the absorber. However, the transmission coefficient shows a noticeable effect due to the change in base thickness, as attenuation is directly related to the path length or base thickness. The tolerance in sphere diameter has resulted in a few dB change in the reflection coefficient, and almost no noticeable change in the transmission coefficient. This can be attributed to the fact that the sphere diameter is related to the introduction of the absorber material into the air, which affects the reflection process.

4. REFLECTION FROM CONDUCTOR-BACKED ABSORBERS

Numerous anechoic chambers are specifically designed to block electromagnetic waves from the chamber to the outside and in the opposite direction. In such setups, the walls are generally lined with conducting sheets, and absorbers are positioned on these conductive surfaces. Therefore, the testing of devices or systems inside the chamber will not be affected by interferences from sources outside the chamber, and at the same time, the performed tests are prevented from affecting nearby systems. This arrangement can be represented by placing a conducting plane underneath the absorber. The modeling was conducted using CST Microwave Suite, in which a conducting plate is positioned under the absorber, as illustrated in Fig. 11. The simulation results of the shielded unit cell are shown in Fig. 12 when the conducting plate was considered to be 35 µm copper and 1 mm iron. The incident wave was applied to port 1, while port 2 was short-circuited

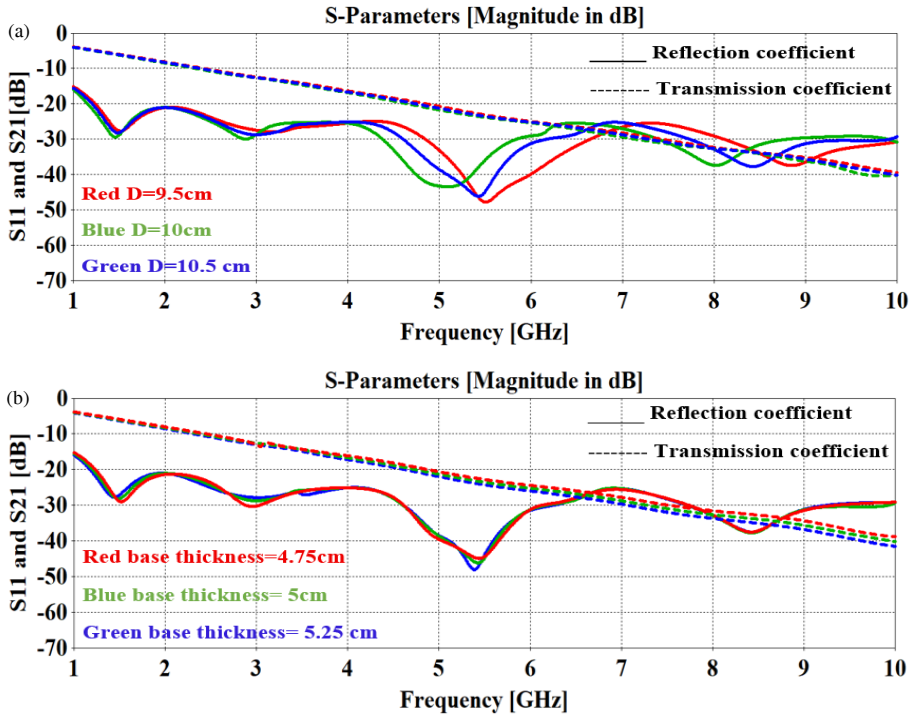

FIGURE 10. Variation of the reflection and transmission coefficients with frequencies for a half sphere absorber with $\varepsilon_r = 1.5$, $\tan\delta = 0.5$. (a) Base thickness of 5 cm for sphere diameters of 9.5, 10, and 10.5 cm, (b) Sphere diameter of 10 cm, for base thickness of 4.75, 5, and 5.25 cm.

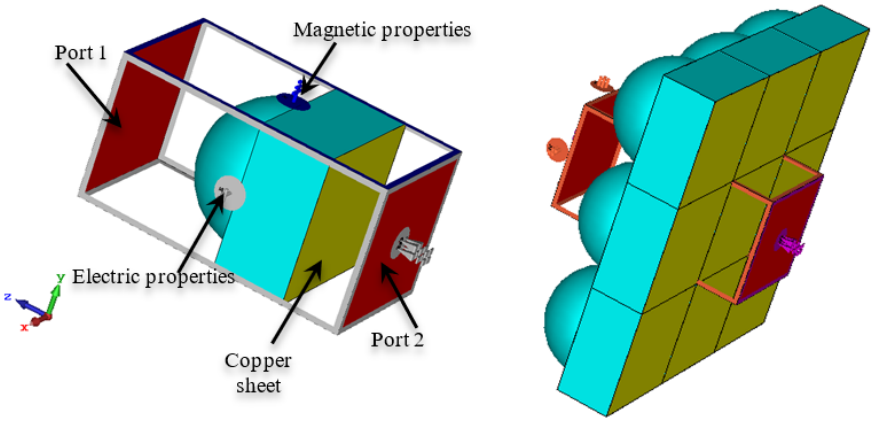

FIGURE 11. The simulation model with a copper sheet placed below the pyramidal absorber.

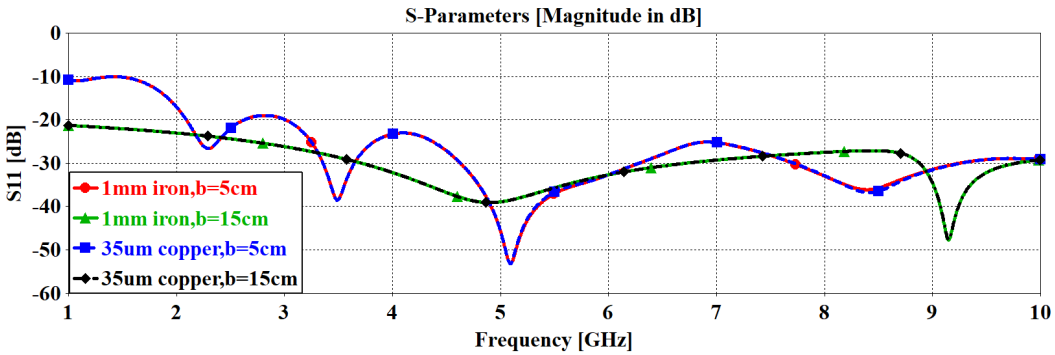

FIGURE 12. The variation of the reflection coefficient $|S_{11}|$ with a frequency for sphere diameter of 10 cm, $\varepsilon_r = 1.5$, and $\tan\delta = 0.5$ at normal incidence, when the conducting plate is 35 μm copper, 1 mm iron for each base thickness 5, and 15 cm.

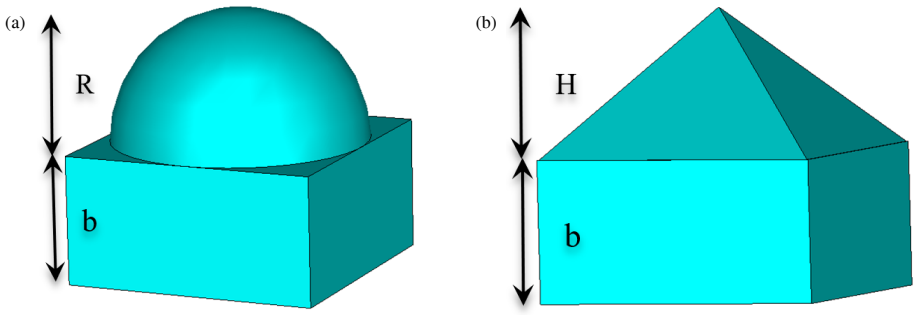

FIGURE 13. Comparison between the half-sphere (a) and pyramidal (b) absorbers.

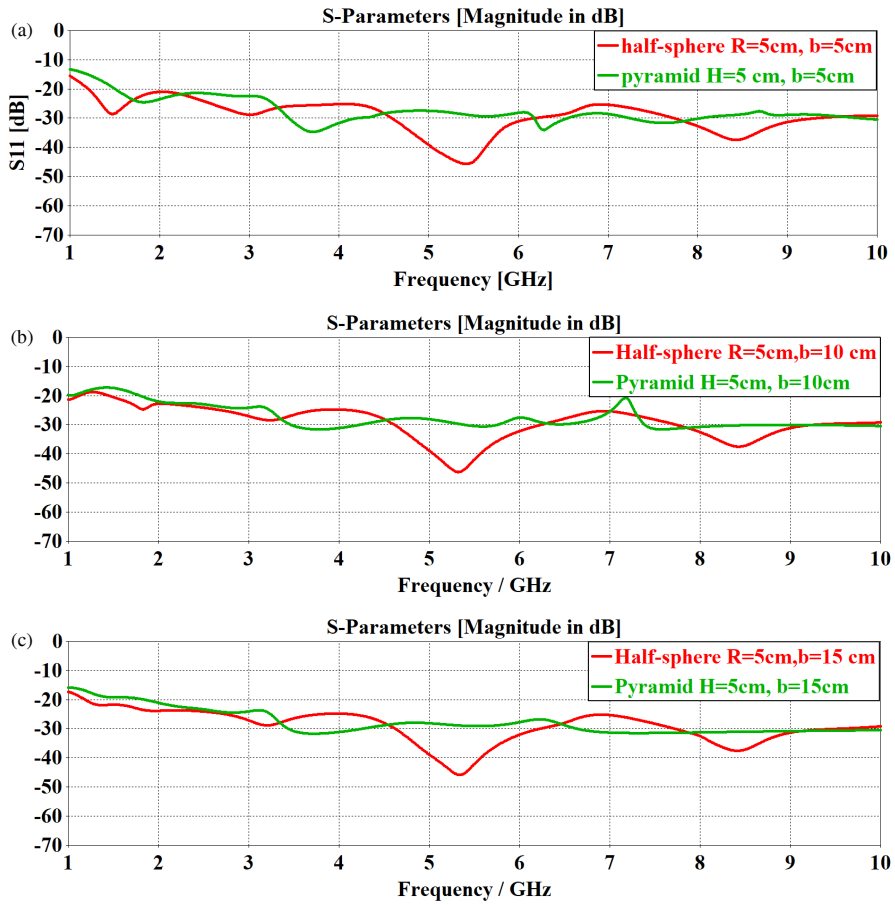

FIGURE 14. Comparison between the variations of the reflection coefficient $|S_{11}|$ with frequency for a half-sphere absorber and the pyramidal absorber, with radius R equal to the pyramid height $H = 5\,\text{cm}$, $\varepsilon_r = 1.5$, and $\tan\delta = 0.5$. (a) $b = 5\,\text{cm}$, (b) $b = 10\,\text{cm}$, and (c) $b = 15\,\text{cm}$.

by the conducting plane. Unit cell boundary conditions were adopted, and a frequency domain solver was used for calculations. It can be seen that for either of the base thicknesses the reflections from the copper-backed absorber and iron-backed absorber are the same. This can be attributed to the fact that the skin depth at 1 GHz for copper is 2.06 µm, which is much smaller than 35 µm, and for iron the skin depth is 4.93 µm which is much smaller than 1 mm. The other note is that the base thickness of 15 cm has reduced the reflection by about 10 dB across the lower half of the shown frequency range compared to the case when the base layer was 5 cm thick. As there is a reflecting plane at the bottom of the absorber, the base thickness has a double-action on the wave that propagates forward and back in the base layer.

5. COMPARISON BETWEEN HALF-SPHERE AND PYRAMID DESIGNS

It is worth comparing the performance of the proposed hemisphere absorber with a pyramidal absorber using the same square base layer and overall thickness as illustrated in Fig. 13. For this fair condition, the hemisphere's radius R was set equal to the pyramid's height H, and the variation of the reflection coefficient with frequency was determined for three values of

TABLE 4. Performance comparison of the proposed absorber with other published works operating at similar frequency bands.

Ref.	Lossy Material	Dimensions [cm]	Frequency Range [GHz]	ε_r	$\tan\delta$	Average S_{11} [dB]	Reflection/ Thickness [dB/cm]
[10]	Ceramic 0-SC	Pyramid $10*10*25$	1–12	2.2	0.34	Maximum about -7 minimum about -40	-0.28 -1.6
[14]	Carbon	Base $5*5*2$, Pyramid $5*5$ base to $1*1$ top with a 12 cm height	1–10	2.5	N.A.	-25.99	-1.85
[22]	Aramid honeycomb coated by a conductive polymer, PEDOT	8.5 cm thick	5.8–18	1.3	Out-of-plane polarization: $\tan\delta \approx 1.7$	Around -10 dB	-1.1
					In-plane polarization: $\tan\delta \approx 1.1$	Around -17 dB	-2
[26]	Carbon	Base $10*10*5$, Pyramidheight 16	1–10	2.5	0.5	-52.6	-2.5
[26]	Carbon	Base $10*10*5$, Pyramidheight 16	1–10	1.5	0.5	-56.66	-2.7
[26]	Carbon	Base $10*10*5$, Pyramidheight 24	1–10	2.5	0.5	-66.5	-2.3
This work	Carbon	Base $10*10*5$ Pyramid $H=5$	1–10	1.5	0.5	-27.5	-2.75
This work	Carbon	Base $10*10*5$ Half sphere $R=5$ cm	1–10	1.5	0.5	-29.5	-2.95
This work	Carbon	Base $10*10*10$ Half sphere $R=5$ cm	1–10	1.5	0.5	-29.1	-1.94
This work	Carbon	Base $10*10*15$ Half sphere $R=5$ cm	1–10	1.5	0.5	-29.2	-1.46

the base thickness. Fig. 13 shows the obtained results, where for $R = 5$ cm, $H = 5$ cm, and a base thickness of 5 cm, the two absorbers exhibit similar performance, while the average reflection coefficient for the half-sphere absorber is -29.5 dB, and that for the pyramid one is higher at -27.5 dB. As the base thickness was increased to 10 cm and 15 cm, the behavior of the half-sphere absorber is still in the average value metric.

6. VERIFICATION USING HFSS SOFTWARE PACKAGE

Instead of the experimental verification, another simulation of the absorber was carried out using Ansoft HFSS software package, where the same absorber parameters used in the CST simulation were submitted to the HFSS model. In particular, the permittivity and loss tangent used in the CST simulations were applied to the HFSS model to ensure fair comparison. The obtained results from the two software packages are compared as shown in Fig. 15. The HFSS results show very close agreement with the CST ones.

7. COMPARISON WITH THE OTHER PUBLISHED WORKS

For further assessment of the performance of the proposed absorber, it is compared here with other designs published in the literature. Table 4 lists a few designs that share the same or similar frequency range, comparable sizes, permittivity, and loss tangent. The suggested comparison metrics are the average value of the reflection coefficient and the efficacy of the reflection measured in attainable reflection/absorber thickness expressed in units of dB/cm. Therefore, the absorber that has a larger absolute value of dB/cm means that it offers lower reflection for a certain value of thickness. By such a definition, the differences in the thickness of the compared absorbers are excluded.

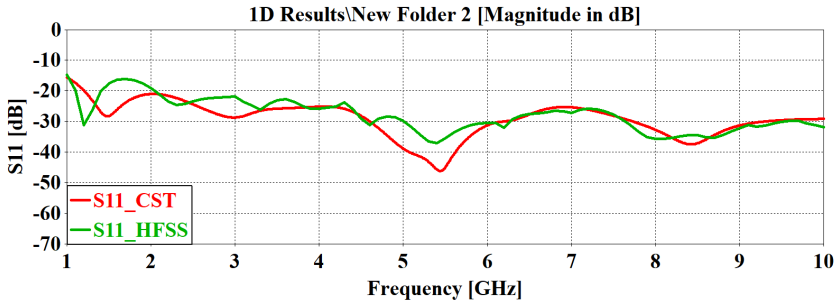

FIGURE 15. The results of the HFSS are compared to those obtained from the CST, for the absorber with a sphere diameter of 10 cm, base thickness of 5 cm, $\varepsilon_r = 1.5$, and $\tan\delta = 0.5$.

The common feature of the compared absorbers is the decrease of the reflection coefficient as the frequency of the incident wave is increased. This demonstrates the difficulty of achieving an adequate level of reflection at lower frequencies. The table shows that the proposed half-sphere absorber offers better values of dB/cm than the designs in [10, 14, 22, 26].

8. CONCLUSIONS

A hemisphere with a square base was chosen to provide a gradual introduction of an absorber into the air while avoiding protrusions and sharp corners that could contribute to reflectivity. The effects of permittivity, loss tangent, hemisphere diameter, base thickness, angle of incidence, and polarization of the incident wave were investigated. Furthermore, this absorber was investigated by supporting it with an iron or copper conductive plate beneath the base to simulate shielded anechoic chamber applications. It was analytically proven through computer simulations that the reflectivity decreases with decreasing permittivity and increasing loss tangent. Additionally, the results showed that the hemisphere is less affected by changing the angle of incidence due to the symmetry of the spherical surface. The comparison of the hemispherical and pyramidal absorbers at the same total thickness showed that the semisphere absorber achieved lower reflection by 2 dB, for angles of incidence up to 20°, while both show lower performance at higher angles. The results obtained from CST were verified by the comparison with those obtained from HFSS simulations. The analysis and obtained results can help designers consider the proposed structure for enhancing the absorber performance.

REFERENCES

[1] Tirkey, M. M. and N. Gupta, "The quest for perfect electromagnetic absorber: A review," *International Journal of Microwave and Wireless Technologies*, Vol. 11, No. 2, 151–167, 2019.

[2] Elmahaishi, M. F., R. S. Azis, I. Ismail, and F. D. Muhammad, "A review on electromagnetic microwave absorption properties: Their materials and performance," *Journal of Materials Research and Technology*, Vol. 20, 2188–2220, Sep.-Oct. 2022.

[3] Abu Sanad, A. A., M. N. Mahmud, M. F. Ain, M. Hussien, M. A. B. Ahmad, Z. M. Ariff, and N. Z. Yahaya, "The prospect of using hollow pyramidal microwave absorbers for 5G anechoic chamber applications: A review," *Journal of Applied Physics*, Vol. 136, No. 23, 230701, 2024.

[4] Jain, P., A. K. Singh, J. K. Pandey, S. Bansal, N. Sardana, S. Kumar, N. Gupta, and A. K. Singh, "An ultrathin compact polarization-sensitive triple-band microwave metamaterial absorber," *Journal of Electronic Materials*, Vol. 50, 1506–1513, 2021.

[5] Jain, P., H. Chhabra, U. Chauhan, K. Prakash, A. Gupta, M. S. Soliman, M. S. Islam, and M. T. Islam, "Machine learning assisted hepta band thz metamaterial absorber for biomedical applications," *Scientific Reports*, Vol. 13, No. 1, 1792, 2023.

[6] Jain, P., M. T. Islam, and A. S. Alshammari, "Comparative analysis of machine learning techniques for metamaterial absorber performance in terahertz applications," *Alexandria Engineering Journal*, Vol. 103, 51–59, 2024.

[7] Simón, J., J. Villanueva, I. A. Arriaga-Trejo, J. R. Flores-González, J. L. Alvarez-Flores, E. S. Hernández-Gómez, R. Piña, and J. Flores-Troncoso, "Evaluation of coir as microwave absorber," *Microwave and Optical Technology Letters*, Vol. 58, No. 6, 1450–1453, Jun. 2016.

[8] Pattanayak, S. S., S. H. Laskar, and S. Sahoo, "Design and development of banana leaves-based double-layer microwave absorber," *IETE Journal of Research*, Vol. 69, No. 2, 924–931, 2023.

[9] Kaur, R., G. D. Aul, and V. Chawla, "Improved reflection loss performance of dried banana leaves pyramidal microwave absorbers by coal for application in anechoic chambers," *Progress In Electromagnetics Research M*, Vol. 43, 157–164, 2015.

[10] Nuan-on, A., N. Angkawisittpan, N. Piladaeng, A. Phankam, N. Tiabpat, and P. C. Ooi, "Design and fabrication of microwave absorbers using water hyacinth," *Engineering Access*, Vol. 3, No. 1, 7–10, 2017.

[11] Rosli, N. S., H. Abdullah, L. M. Kasim, S. Abdullah, M. N. Taib, S. M. M. Kasim, N. M. Noor, and A. Ahmad, "Pyramidal microwave absorbers: Leveraging ceramic materials for improved electromagnetic interference shielding," *International Journal of Electrical & Computer Engineering (2088-8708)*, Vol. 15, No. 1, 435–447, 2025.

[12] Kaur, H., G. D. Aul, and V. Chawla, "Enhanced reflection loss performance of square based pyramidal microwave absorber using rice husk-coal," *Progress In Electromagnetics Research M*, Vol. 43, 165–173, 2015.

[13] Houbi, A., Z. A. Aldashevich, Y. Atassi, Z. B. Telmanovna, M. Saule, and K. Kubanych, "Microwave absorbing properties of ferrites and their composites: A review," *Journal of Magnetism and Magnetic Materials*, Vol. 529, 167839, 2021.

[14] Nornikman, H., P. J. Soh, A. A. H. Azremi, and M. S. Anuar, "Performance simulation of pyramidal and wedge microwave absorbers," in *2009 Third Asia International Conference on*

Modelling & Simulation, 649–654, Bundang, Indonesia, May 2009.

[15] Nornikman, H., F. Malek, P. J. Soh, A. A. H. Azremi, and A. Ismahayati, "Reflection loss performance of triangular microwave absorber," in *International Symposium on Antennas and Propagation (ISAP 2010)*, 2010.

[16] Nornikman, H., P. J. Soh, and A. A. H. Azremi, "Performance of different polygonal microwave absorber designs using novel material," in *The 2009 International Symposium on Antennas and Propagation (ISAP 2009)*, 1151–1154, Bangkok, Thailand, Oct. 2009.

[17] Nornikman, H., F. Malek, P. J. Soh, and A. A. H. Azremi, "Reflection loss performance of hexagonal base pyramid microwave absorber using different agricultural waste material," in *2010 Loughborough Antennas & Propagation Conference*, 313–316, Loughborough, UK, Nov. 2010.

[18] Catalkaya, I. and S. Kent, "An optimized microwave absorber geometry based on wedge absorber," *Applied Computational Electromagnetics Society Journal (ACES)*, Vol. 32, No. 7, 621–627, 2017.

[19] Bağmancı, M., L. Wang, C. Sabah, M. Karaaslan, L. C. Paul, T. Rani, and E. Unal, "Broadband multi-layered stepped cone shaped metamaterial absorber for energy harvesting and stealth applications," *Engineering Reports*, Vol. 6, No. 11, e12903, 2024.

[20] Yusof, A. S., H. Abdullah, N. R. A. A. Fauzi, N. A. Ismail, A. R. Razali, A. Ahmad, M. N. Taib, A. Azmin, N. M. Kasim, and A. M. Mozi, "Slotted triangle on hollow pyramidal microwave absorber characteristics," in *2016 6th IEEE International Conference on Control System, Computing and Engineering (ICCSCE)*, 563–568, Penang, Malaysia, 2016.

[21] Asmadi, M. F., H. Abdullah, M. N. Taib, M. I. Fazin, A. Ahmad, N. M. Kasim, N. A. Ismail, and M. M. Jumidali, "The optimal performance of a geopolymer hollow pyramidal microwave absorber with triangular slotted," *Solid State Phenomena*, Vol. 344, 97–102, Jun. 2023.

[22] Choi, J.-H., M.-S. Jang, W.-H. Jang, and C.-G. Kim, "Investigation on microwave absorption characteristics of conductive-coated honeycomb absorber," *Composite Structures*, Vol. 242, 112129, 2020.

[23] Zhang, W., R. Mi, and V. Khilkevich, "3D printed multilayer microwave absorber," in *2022 IEEE International Symposium on Electromagnetic Compatibility & Signal/Power Integrity (EMCSI)*, 59–63, Spokane, WA, USA, 2022.

[24] Hasar, U. C., Y. Kaya, H. Korkmaz, and T. Iliev, "Broadband multilayer absorber design using double-stage cognitive seeker optimization algorithm," *IEEE Access*, Vol. 13, 27 178–27 190, 2025.

[25] Zong, Y. M., W. B. Kong, J. P. Li, L. Wang, H. N. Zhang, F. Zhou, and Z. Y. Cheng, "Optimization of multilayer microwave absorbers using multi-strategy improved gold rush optimizer," *Applied Computational Electromagnetics Society Journal (ACES)*, Vol. 39, No. 8, 708–717, Aug. 2024.

[26] Thanoon, A. R. and K. H. Sayidmarie, "Analysis of pyramidal microwave absorbers for enhanced performance in 1-10 GHz frequency range," *Journal of Telecommunications and Information Technology*, No. 2, 29–37, 2025.

[27] Duan, Y. and H. Guan, *Microwave Absorbing Materials*, Jenny Stanford Publishing, 2016.

[28] Hofmann, W., A. Schwind, C. Bornkessel, and M. A. Hein, "Angle-dependent reflectivity of microwave absorbers at oblique wave incidence," in *2021 51st European Microwave Conference (EuMC)*, 233–236, London, United Kingdom, 2022.

[29] Lin, F., Y. Bai, J. Chen, Z. Yan, H. Zhou, and Y. Wang, "Flexible and broadband microwave-absorbing metastructure with wide-angle stability," *Journal of Applied Physics*, Vol. 136, No. 23, 233101, 2024.